中國機械工程學刊第四十卷第三期第 221~229 頁(民國一百零八年)
Journal of the Chinese Society of Mechanical Engineers, Vol.40, No.3, pp 221~229 (2019)

Virtual Prototype and Experiment Study on Mining Truck Air Brake System

Xiaobin Fan*and Zeng Song**

Keywords: mining dump truck, virtual prototype, service brake, emergency brake, retarder, air brake.

ABSTRACT

Accurate calculation method of drum brake braking torque of mining truck air brake was studied in this paper at first, then hydro pneumatic suspension features and the tire characteristic parameters were studied. The dump truck virtual prototype model was established, service brake and emergency brake performance were simulated. The simulation results of braking deviation show that the rear wheel braking force is greater than that the front wheel. Under cornering braking condition, the brake deviation increases about 85 mm for each 5% difference between the left and right brake forces of the front wheel; 5% difference between the left and right brake forces of the rear wheel, the brake deviation increases about 120 mm. Braking locking sideslip simulation shows that when the front wheel is locked, the side slip of the vehicle deviates from the track up to 2m, which is very dangerous in the mountain mining area. The truck performance field tests were carried out such as service brake, emergency brake, hydraulic retarder and brake system response time, etc. The results show that the truck braking performance can also be improved. Because braking pressure rise time is slightly long, that it can be improved by gas circuit improvement (equipped with the quick-acting valve and wet-road valve, etc.), and the superiority of the improved gas path is also verified by virtual prototype simulation and real vehicle experiment. The truck braking torque can be further promoted by increasing air pressure or brake friction coefficient or brake design rationality. Through the implementation of these methods, the braking performance of the mine dump truck has been improved significantly.

INTRODUCTION

Mining dump truck is widely used in mining and infrastructure areas. Due to its poor driving conditions and large capacity, it must have a very stable and reliable braking system (SAE, 1990). Maxym (2014) proposed an algorithm of ABS modulators controller for truck, but they only has carried out by simulation analysis, not proceeded real vehicle experiment, the actual control effect need to be examined. S.Mithun (2014) described the detailed modeling of the individual brake system products, right from the actuating valves, control valves, actuators and foundation brakes. Response time prediction for a typical 4×2 Heavy commercial vehicle has been done. Also a study on comparing the transient torque generated by the existing drum brake and an equivalent disc brake model was carried out, but he did not carry out vehicle braking performance experiments in the paper. Subhajit (2009) developed a mathematical model for the overall longitudinal dynamic response of a commercial vehicle equipped with an electropneumatic braking system. Selim (2012) examined the computer-aided vehicle dynamics analysis of a 6×2 heavy-duty commercial vehicle by Mechanical Simulation Corporation's Truck-Sim multibody dynamics simulation and SuspensionSim multibody statics simulation softwares, but they only has carried out the vehicle dynamics simulation analysis and have not carried out the response characteristics of the braking system for experiments. D. B. Sonawane (2011) presented a mathematical model for the mechanical subsystem of the air brake system that can be used to monitor the clearance between the brake shoe/pad and the brake drum. This mathematical model correlates the push rod stroke transients and the brake chamber pressure transients. A kinematic analysis and a dynamic analysis of the mechanical subsystem of the air brake system were performed, and the results were corroborated with experimental data, but they have not carried out the response characteristics experiments of the entire pneumatic brake system. Shimanovsky (2016) analyzed the influence of spring stiffness and wheel weight on partially filled tanker truck oscillations at braking. Li (2015) introduced the configuration and operation principle of the hydraulic in-wheel motor drive system for heavy truck. Hemant (2016) implemented stress analysis and predicted life of front axle for vertical and braking loading case using analytical, experimental and FEA method. Daniel (2016) carried out analysis of truck braking system in terms of construction and operation.

VIRTUAL PROTOTYPE MODELING

Drum Brake Model Analysis

The truck front and rear brake are drum brake with internal expansion shoe (normal pressure is 0.86MPa). Front and rear brakes circuit are independent and controlled by foot valve and auxiliary handbrake valve. When driving on slippery roads, the driver can open the wet/dry road valve, which can make the front wheel

Paper Received February, 2018. Revised December, 2018. Accepted March, 2019. Author for Correspondence:Xiaobin Fan.

**Associate Professor, School of Mechanical and Power Engineering, Henan Polytechnic University, 454000 Jiaozuo, China*

***Graduate Student, School of Mechanical and Power Engineering, Henan Polytechnic University, 454000 Jiaozuo, China*

brake pressure reduce half, thus keeping direction stability under Braking-In-Turn. The alarm indicator will light up in driving indoor when the system pressure reduces to 550kPa. If the system pressure reduces to 310kPa, the truck front and rear brake will work automatically (Zhang, 2008). Parking brake will work when operating Parking brake switch on manipulation dashboard. The torque calculation process of pneumatic drive drum brake is as follows.

(1)The force Ce and Ct acting on leading and trailing shoe of brake

Brake chamber pressure acts on leading and trailing shoe by slack adjuster and cam shaft, as shown in Fig.1. Brake chamber thrust force Q is as follows.

$$Q = \pi (d/2)^2 p \tag{1}$$

where, d is effective diameter of brake chamber, p is brake chamber pressure. By the force balance acting on the cam, there are equations as follows.

$$Q \cdot rc = (Ce + Ct) \cdot \left(\frac{Dg}{2} + Uc \cdot S \right) \tag{2}$$

$$Ce + Ct = \frac{Q \cdot rc}{\frac{Dg}{2} + Uc \cdot S} \tag{3}$$

where, rc is the length of the cam leverage (here, refers to the length of the slack adjusters); Dg is cam base circle diameter; Uc is the friction coefficient between the cam and roller, and Uc=0.1; S is shown in Fig.1; Ce is the cam driving force on tight shoes; Ct is the cam driving force on hoof shoes.

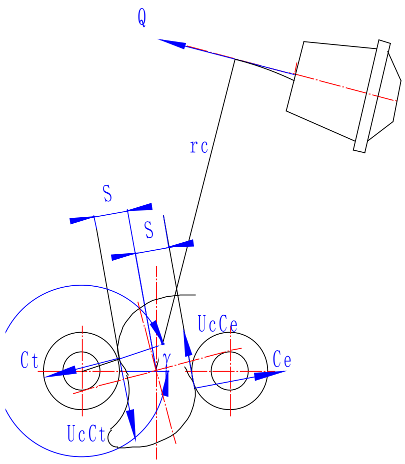

Fig.1 Brake force diagram

(2) The friction force of per unit area

The plate friction force is shown in Fig.2. According to the moment balance, there have equations as follows.

For leading shoe

$$Ce \cdot me - Ue \cdot Ce \cdot ne = \int_{\theta 1}^{\theta 2} Pe \cdot B \cdot rd \cdot l \cdot \sin^2 \theta d\theta - \int_{\theta 1}^{\theta 2} UePe \cdot B \cdot rd (rd - l\cos\theta) \sin\theta d\theta \tag{4}$$

For trailing shoe

$$\begin{aligned} Ct \cdot mt - Uc \cdot Ct \cdot nt = & \left\{ \int_{\theta 1}^{\theta 2} Pt \cdot B \cdot rd \cdot l \sin^2\theta d\theta + \int_{\theta 1}^{\theta 2} UePt \cdot B \cdot rd (rd - l\cos\theta)\sin\theta d\theta \right\} \\ & - \left\{ Pt \cdot b \cdot rd \cdot l \left(\int_{\varphi 1}^{\varphi 2} \sin^2\varphi d\varphi + \int_{\varphi 3}^{\varphi 4} \sin^2 \varphi d\varphi \right) + UePt \cdot b \cdot rd \left(\begin{aligned} & \int_{\varphi 1}^{\varphi 2} (rd - l\cos\varphi)\sin\varphi d\varphi \\ & + \int_{\varphi 3}^{\varphi 4} (rd - l\cos\varphi)\sin\varphi d\varphi \end{aligned} \right) \right\} \end{aligned} \tag{5}$$

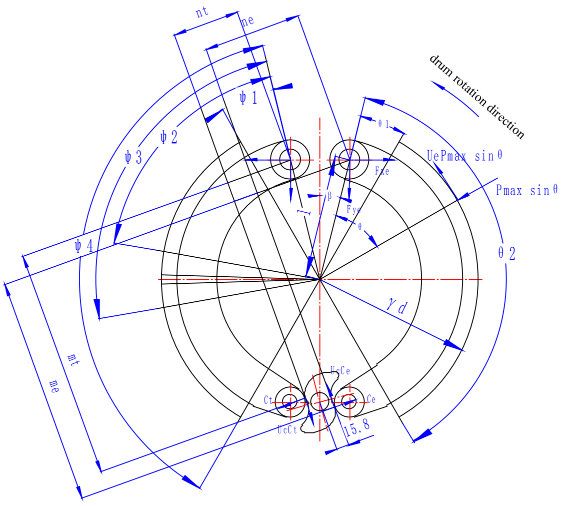

Fig.2 The friction plate force diagram

where, B is the friction plate width (mm); b is the width of the friction plate grooving (mm); rd is the radius of the drum (mm); Ue is the friction coefficient of friction plate; Pe is turn tight shoe maximum pressure per unit area (Kg/mm^2); Pt is turn loose shoe pressure per unit area (Kg/mm^2); $\theta 1$ and $\theta 2$ are friction plate position angle; $\psi 1$, $\psi 2$, $\psi 3$ and $\psi 4$ are the angle of the friction plate grooving position; me, mt, ne, nt and l are shown in Fig. 3; r is effective radius of brake chamber.

Because the cam has a fixed axis, so friction should be equal of turn tight shoe and turn loose shoe on the geometry, thus the maximum pressure per unit area of the friction piece should be equal (Wong, 2001). Namely: Pe=Pt=P. X, Y, Z, U, V and W are set as follows.

$$X = \int_{\theta 1}^{\theta 2} \sin^2\theta d\theta = \frac{\theta_2 - \theta_1}{2} - \frac{\sin 2\theta_2 - \sin 2\theta_1}{4}$$

$$Y = \int_{\theta 1}^{\theta 2} \sin\theta \cos\theta d\theta = \frac{\cos 2\theta_1 - \cos 2\theta_2}{4}$$

$$Z = \int_{\theta 1}^{\theta 2} \sin\theta d\theta = \cos\theta_1 - \cos\theta_2$$

$$U = \int_{\varphi 1}^{\varphi 2} \sin^2 \varphi d\varphi + \int_{\varphi 3}^{\varphi 4} \sin^2\varphi d\varphi = \frac{(\varphi_2 - \varphi_1) + (\varphi_4 - \varphi_3)}{2} - \frac{(\sin 2\varphi_2 - \sin 2\varphi_1) + (\sin 2\varphi_4 - \sin 2\varphi_3)}{4}$$

$$V=\int_{\varphi1}^{\varphi2}\sin\varphi\cos\varphi d\varphi+\int_{\varphi3}^{\varphi4}\sin\varphi\cos\varphi d\varphi=\frac{\left(\cos2\varphi_1-\cos2\varphi_2\right)+\left(\cos2\varphi_3-\cos2\varphi_4\right)}{4}$$

$$W=\int_{\varphi1}^{\varphi2}\sin\varphi d\varphi+\int_{\varphi3}^{\varphi4}\sin\varphi d\varphi=\cos\varphi_1-\cos\varphi_2+\cos\varphi_3-\cos\varphi_4$$

So, the simplified form of *Ce* and *Ct* can be got as follows.

$$Ce=\frac{B\cdot rd\left\{l\cdot X-Ue(rd\cdot Z-l\cdot Y)\right\}}{me-Ue\cdot ne}\cdot P \tag{6}$$

$$Ct=\left\{\frac{B\cdot rd\left[l\cdot X+Ue\left(rd\cdot Z-l\cdot Y\right)\right]-b\cdot rd\left[l\cdot U+Ue\left(rd\cdot W-l\cdot V\right)\right]}{mt-Uc\cdot nt}\right\}\cdot P \tag{7}$$

From equation (3), equation (6) and equation (7), the following equation can be obtained.

$$P=\frac{\dfrac{Q\cdot rc}{\dfrac{Dg}{2}+Uc\cdot S}}{rd\left\{\dfrac{B\left[l\cdot X-Ue(rd\cdot Z-l\cdot Y)\right]}{me-Uc\cdot ne}+\dfrac{B\left[l\cdot X+Ue(rd\cdot Z-l\cdot Y)\right]-b\left[l\cdot U+Ue(rd\cdot W-l\cdot V)\right]}{mt-Uc\cdot nt}\right\}} \tag{8}$$

(3) The brake torque

Leading shoe brake torque is as follows.

$$Te=\int_{\theta1}^{\theta2}UePB(rd)^2\sin\theta d\theta=UePB(rd)^2Z \tag{9}$$

Trailing shoe brake torque is as follows.

$$Tt=UeP(rd)^2\left\{B\int_{\theta1}^{\theta2}\sin\theta d\theta-b\left[\int_{\varphi1}^{\varphi2}\sin\varphi d\varphi+\int_{\varphi3}^{\varphi4}\sin\varphi d\varphi\right]\right\}=UeP(rd)^2(BZ-bw) \tag{10}$$

The total brake torque is as follows.

$$M_b=UeP[B(rd)^2Z+(rd)^2(BZ-bw)]\cdot\eta$$

where, η is braking efficiency reduction factor considered the cam lever tilt and relative moving parts friction, etc. Here, η=0.8.

The front and rear brake parameter are shown in Table 1 and Table 2. Substituting parameters into equations, we can obtain front and rear brake torque constant as 23487 N·m/MPa and 41264 N·m/MPa respectively. According to the test results (Fig. 8), front brake system pressure is 0.63 MPa, clearance elimination time is 0.1s, air pressure rise time is 0.95s; The rear brake system pressure is 0.64MPa, clearance elimination time is 0.1s, air pressure rise time is 0.35s. Front and rear brake system braking torque are 29594N·m and 52819N·m respectively.

Table 1. Front brake parameters

parameter	value	parameter	value
r (mm)	205	ψ_1 (º)	13
r_c (mm)	160.47	ψ_2 (º)	87
D_g (mm)	26.2	ψ_3 (º)	91
r_d (mm)	254	ψ_4 (º)	144
B (mm)	152	θ_1 (º)	13
U_e	0.3	θ_2 (º)	144
U_c	0.1	m_e (mm)	334.3
b (mm)	21	m_t (mm)	315.6
S (mm)	13.4	n_e (mm)	267.5
l (mm)	214.3	n_t (mm)	240.7

Table 2. Front brake parameters

parameter	value	parameter	value
r (mm)	205	ψ_1 (º)	8
r_c (mm)	171.5	ψ_2 (º)	74
D_g (mm)	26.2	ψ_3 (º)	78
r_d (mm)	254	ψ_4 (º)	141
B (mm)	190	θ_1 (º)	8
U_e	0.3	θ_2 (º)	141
U_c	0.1	m_e (mm)	334.3
b (mm)	21	m_t (mm)	315.6
S (mm)	13.4	n_e (mm)	267.5
l (mm)	206.2	n_t (mm)	240.7

Hydro-Pneumatic Suspension Structure and Parameters Calculation

The front and rear suspension adopts helium/oil variable ratio self-contained cylinder, it deliveries pressure by the oil uses inert gas nitrogen as elastic medium. Which is composed of energy accumulator (gas spring) and suspension cylinder with shock absorber function. Suspension installation and structure diagram are shown in Fig.3 (a) and Fig.3 (b) respectively. Among them, the biggest impact stroke of front suspension is 225 mm, maximum impact stroke of rear suspension is 160 mm.

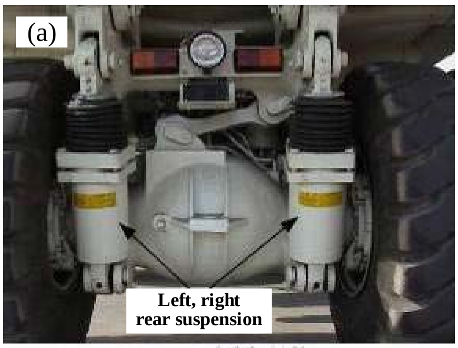

(b)

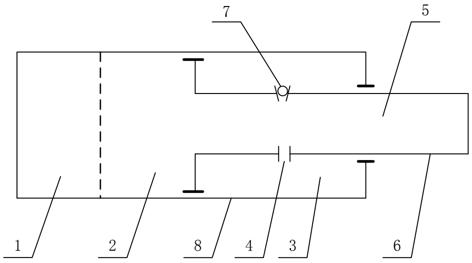

Fig.3 Suspension cylinder installation and structure
1- air cavity A; 2-fluid cavity B; 3- fluid cavity C; 4- damping hole; 5- fluid cavity D; 6- rod cylinder; 7- one-way valve; 8- cylinder

When rod cylinder 6 enters cylinder 8, nitrogen in air cavity A is compressed and stores energy, and when stretching out, nitrogen in air cavity A is expanded and releases energy. When rod cylinder has reciprocating motion, the volume of fluid cavity C is changing, the volume C increasing when rod cylinder comes into, and the oil flow comes into the B and D cavity from C. C cavity volume decreases when stretching out, and the oil is discharged to B and D cavity. Oil discharge and supplement relies on the damping hole 4 and one-way valve 7, so as to control the speed of the hydraulic reciprocating flow and produce certain damping effect. This damping effect will consume energy and have the effect as a two-way shock absorber. When the rod cylinder stretches out, only the damping hole 4 works and the flow area is small and the damping effect increases. When the rod cylinder comes into, damping hole 4 and one-way valve 7 work at the same time, the damping effect is less, and the suspension damping function mainly relies on the elastic effect of the gas. The output force of hydro pneumatic suspension is mainly composed of gas elastic force F_g, the oil damping force F_c and friction force under the external excitation (Yibin Wang,2005; Decheng Zhou, 2005). The friction force is set to a fixed value 3 kN. Elastic force $F_g(x)$ is calculated by R-K equation, the calculation process is as follows.

$$F_g(x)=\frac{RTA_g}{\frac{P_0V_0/P_s+A_gx}{m/M}-b}-\frac{aA_g}{T^{1/2}[\frac{P_0V_0/P_s+A_gx}{m/M}][\frac{P_0V_0/P_s+A_gx}{m/M}+b]} \tag{11}$$

where, R is the universal gas constant, 296.8 J/kg·K; T is the actual gas absolute temperature, 283.15K; P_0 is initial charge pressure of suspension cylinder, 1.4MPa; V_0 is initial air volume, 0.005m^3; P_s is the gas pressure at balanced position, 3.3481MPa; m is the mass of the gas, 0.0195kg; M is the gas molecular weight, 28.013; A_g is the air cavity cross-sectional area, 0.0154m^2; a and b are constants related to the gas species, 1.5575 and 2.6781×10^5 respectively. x is the rod cylinder displacement relative to the cylinder, the unit is m. Damping force $F_c(v)$ calculation is as follows.

$$F_c(v)\begin{cases}\dfrac{0.3164\rho^{0.75}(\mu_0e^{-\lambda(t-50)})^{0.25}A_c}{2d_s^{1.75}[1+\frac{A_d}{A_s}1.75\sqrt{\frac{L_s}{L_d}[\frac{d_d}{d_s}]^{1.25}}]^{1.75}}[\dfrac{A_cv}{A_s}]^{1.75} & v<0\\ \dfrac{0.3164L_s\rho^{0.75}(\mu_0e^{-\lambda(t-50)})^{0.25}A_c}{2d_s^{1.75}}[\dfrac{A_cv}{A_s}]^{1.75} & v>0\end{cases} \tag{12}$$

where, ρ is the oil density, 850kg/m^3. t is the oil temperature, 10℃; t_0 is the oil temperature, 50℃; μ_0 is the oil power viscosity at t_0, 0.85 Pa·s; λ is the oil viscosity-temperature index, 0.0501; A_s is one-way valve flow area, 0.00005m^3; A_d is damping orifice flow area, 0.00002m^3. L_s is a one-way valve flow length, 0.03m; L_d is damping orifice flow length, 0.03m; d_s is one-way valve hydraulic diameter, 0.004m; d_d is hydraulic damping hole diameter, 0.005m; A_c is the ring cavity cross-sectional area, 0.0073m^2; v is the rod cylinder speed relative to the cylinder, the unit is m/s. The working characteristic test curve of front and rear hydro pneumatic suspension are shown in Fig.4 and Fig.5 respectively, and which will be entered into the virtual prototype model file.

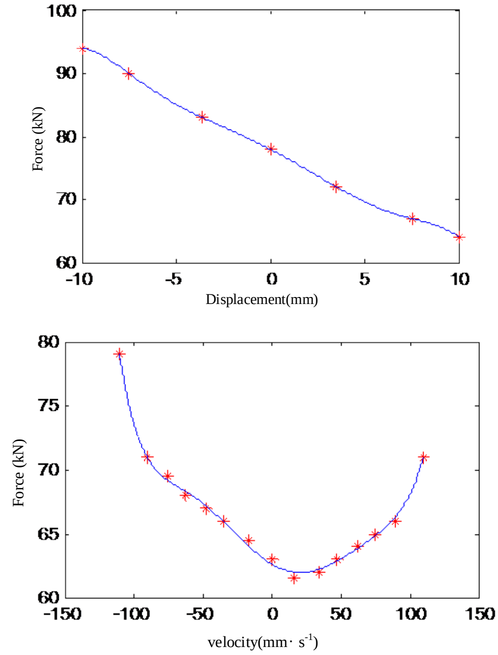

Fig.4 Experimental curve of working characteristics of front suspension (exciting frequency is 1.67 Hz)

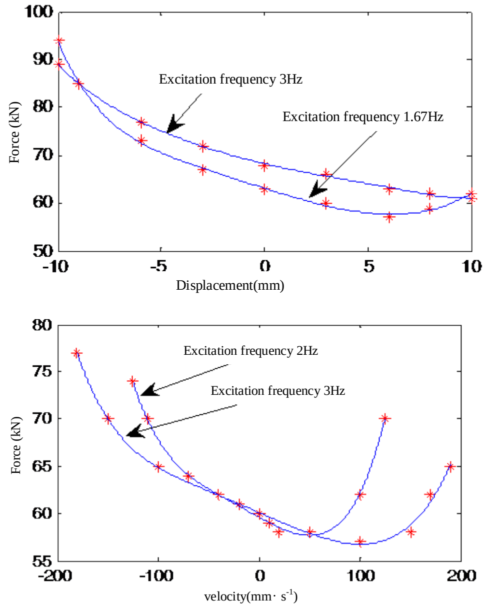

Fig.5 Experimental curve of rear suspension working characteristics

Tire Parameters

The tire model file in MSC. ADAMS consists the following parameters: the UNITS (including length, force, angle, quality, time, etc.), MODEL (MODEL type), R1 (free radius) and R2 (tire crown radius), CNORMAL (radial stiffness), CSLIP (longitudinal slip stiffness) and CALPHA (cornering stiffness), CGAMMA (camber stiffness), CRR (rolling resistance coefficient), RDR (radial relative damping coefficient), U0 (static friction coefficient), U1 (dynamic friction coefficient) (H.B.Pacejka, 2006), the mining truck tire parameters are shown in Table 3.

Table 3. Tire parameters

parameter name	unit	front tire	rear tire
model		18.00-25 28 ply rating E3 tubeless	18.00-25 28 ply rating E3 tubeless
R1	mm	808.5	808.5
R2	mm	317.5	317.5
CN	N/mm	4000	8000
CSLIP	N/mm	15000	30000
CALPHA	N/rad	300000	500000
CGAMMA	N/rad	25000	50000
CRR	none	0.015	0.015
RDR	none	0.7	0.7
U0	none	1.0	1.0
U1	none	0.9	0.9
quality	kg	261*2	261*4
Ixx/Iyy/Izz	kg·mm^2	(4.8,4.8,8.6)e^7	(4.8,4.8,8.6)e^7
section width	mm	495	495*2

Full Vehicle Virtual Prototype Model

According to the manufacturers' drawings, the 3D prototypes of major components were built firstly and these quality and inertia moment are acquired and imported into ADAMS software and assembled. The whole vehicle virtual prototype model is shown in Fig.6. Brake pressure was implemented on the braking system according to the measured results (shown in Fig.7). There were some assumptions made in the modeling process as following: 1) Because the truck speed is small, the effect of wind resistance is ignored; 2) The parts were connected by ideal motion pair, the influence of friction and damping were ignored; 3) Power transmission system was simplified, namely the driving or braking torque was directly applied on revolution joint between the wheel and axle.

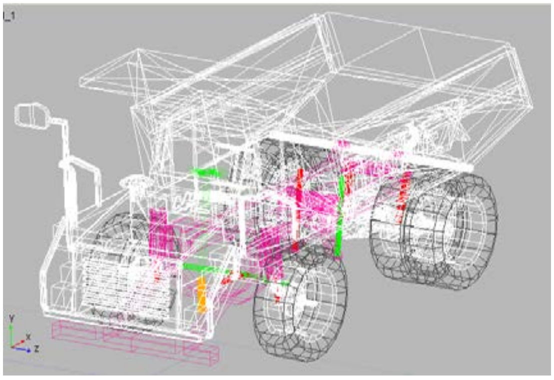

Fig.6 Vehicle virtual prototype model

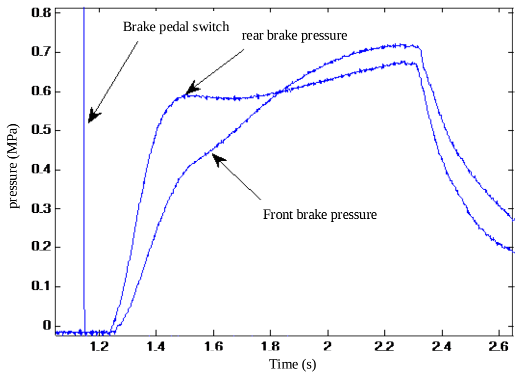

Fig.7 Brake pressure test curve

BRAKING PERFORMANCE VIRTUAL PROTOTYPE SIMULATION

Service Brake Simulation

Substituting field test results, braking performance simulation results on dry concrete pavement (μ is Tire / pavement friction coefficient, μ=0.8) were acquired. It can be seen that the mean fully developed deceleration (MFDD) is 2.155m/s^2 and consistent with real test results (2.156m/s^2); Braking distance is 49.67 m, the braking time is 6.80s, the front wheel slip rate is 0.069, the rear wheel slip rate is 0.062, the front wheel provides the ground braking force as 40.52 kN, the rear wheel provides ground braking force as 68.9 kN, the load transfer is about 32%.

According to SAE J1473, emergency brake standards are: under initial speed of 25km/h and on 9% grade road, the braking distance S_{25_9} is as follows (SAE, 1990).

$$s_{25\_9} = \frac{25^2}{34 - 2.6 \times 0.09} = 18.51\text{m}$$

According to the braking distance calculation formula, there has the following equation.

$$s_{25\_9} = \frac{1}{3.6}\left(\tau_2^{'} + \frac{\tau_2^{''}}{2}\right) \times 25 + \frac{25^2}{25.92 a_{25\_9}} \tag{13}$$

where, $\tau_2^{'}$ is brake clearance elimination time; $\tau_2^{''}$ is brake pressure rise time. The maximum braking deceleration a_{25_9} of standard requirements can be calculated by equation (14) as follows.

$$a_{25\_9} = \frac{25^2}{\left[s_{25\_9} - \frac{1}{3.6}\left(\tau_2^{'} + \frac{\tau_2^{''}}{2}\right) \times 25\right] \cdot 25.92} \tag{14}$$

Due to the field test road as straight, so the standard of average deceleration a_{25_9} should be converted to straight roads as $a_{25\_0} = a_{25\_9} + g \times \sin(arc\tan(0.09))$, that is MFDD should not be more than a_{25_0}.

Braking performance simulation results under various adhesion road are shown in Table 4. We can see the front wheel is locked ahead of the rear on μ=0.25 road, the front and rear wheel are both locked when μ=0.1; Even if the wet road valve is open (front braking torque is in half), the front wheel is still locked when μ=0.09, namely on this road we can't guarantee the direction stability under turning and braking. In this case, ABS(Antilock Brake System) should be installed.

Table 4. Braking performance simulation results

μ	a_v (m/s2)	MFDD (m/s2)	D_b (m)	t_b (s)	F_{bf} (kN)	F_{br} (kN)

0.8	2.033	2.155	49.67	6.80	40.52	68.97
0.5	2.033	2.155	49.67	6.80	40.52	68.97
0.25	1.69	1.73	59.75	8.32	40.4	47.4
0.1	0.62	0.62	151.8	22.23	9.82	21.02

Emergency Brake

When the system pressure drops to 310kPa, front and rear brake mechanism will lock chamber push rod, front and rear brake will work automatically. Namely, the emergency braking torque is equal to the service brake, but system reaction time will become shorter. In this case the front emergency braking torque is 14.56kN and the rear is 25.58kN·m. There are two different conditions: the first is the rear brake circuit failure, the front service brake and the rear emergency brake work at the same time. The other is the front brake circuit failure, the front emergency brake and the rear service brake work at the same time. The simulation results under rear brake circuit failure are shown in Table 5 and the simulation results under front brake circuit failure are shown in Table 6.

Table 5. Simulation results under rear brake circuit failure

μ	a_v (m/s2)	MFDD (m/s2)	D_b (m)	t_b (s)	F_{bf} (kN)	F_{br} (kN)
0.8	1.42	1.55	18.23	4.88	41.8	36.8
0.5	1.42	1.55	18.23	4.88	41.8	36.8
0.2	1.28	1.32	19.5	5.41	30.1	37

Table 6. Simulation results under front brake circuit failure

μ	a_v (m/s2)	MFDD (m/s2)	D_b (m)	t_b (s)	F_{bf} (kN)	F_{br} (kN)
0.8	1.69	1.84	15.2	4.08	22.6	70.9
0.2	1.17	1.23	21.4	5.92	22.4	39.8

The simulation results are basically consistent with the experimental results. In order to improve the braking performance of mine trucks, we have improved the braking efficiency and braking direction stability of the whole truck through the quick-acting valve and the wet road valve respectively.

Braking Deviation Simulation on Straight Road

The braking deviation of flat road braking, front/rear wheel braking force unequal (the left braking force is larger) is simulated at initial braking speed 30km/h. Figure 8 and Table 7 are the simulation result. Among them, the inequality $\Delta F_{\mu r}$ of left and right braking force is as follows.

$$\Delta F_{\mu r} = \frac{F_{\mu b} - F_{\mu l}}{F_{\mu b}} \times 100\%$$

Where, $F_{\mu b}$ is the braking force of the large brake, and $F_{\mu l}$ is the small brake force.

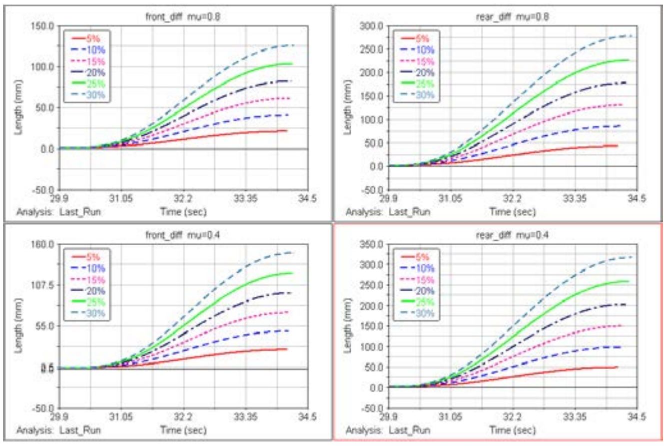

Fig.8 Deviation by unequal braking force of front and rear wheels

Table 7. Deviation by unequal braking force of front and rear wheels (Unit: mm)

	μ	5%	10%	15%	20%	25%	30%
Front wheel left and right unequal	0.8	20.8	40.6	60.9	81.8	103.2	125.2
	0.4	24.4	47.9	71.9	96.6	122	148.1
Rear wheel left and right unequal	0.8	42.3	84.9	129.7	176.7	225.9	277.4
	0.4	48.6	97.6	149	202.6	258	316

The simulation results show that the deviation of the rear wheel braking force is greater than that the front wheel. The simulation results are basically consistent with the experimental results.

Corner Braking Deviation Simulation on Straight Road

The vehicle trajectory was shown in Fig.9 when the front and rear wheels braking force is unequal under the front wheel turns left 4° on μ=0.8 road. The X coordinate is the longitudinal displacement of the vehicle (from right to left is the direction of driving), the Y coordinate is the lateral displacement of the vehicle, and the swa in the figure is steering angle.

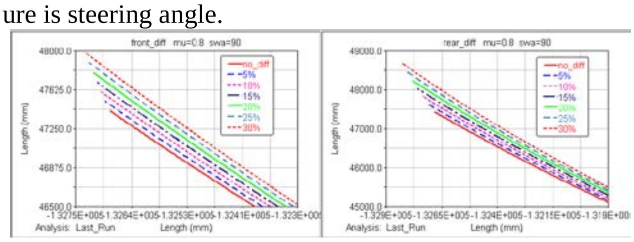

Fig. 9 Vehicle trajectories under turning and braking with left and right unequal braking force of rear wheels

The simulation results show that the brake deviation increases about 85 mm for each 5% difference between the left and right brake forces of the front wheel. 5% difference between the left and right brake forces of the rear wheel, the brake deviation increases about 120 mm. Which are greater than the deviation of the straight brake.

Sideslip Simulation Under Lock Braking

Fig. 10 is the trajectory of vehicle center underside-slipping caused by centrifugal force (lateral force) during front and rear wheel lock braking on steering braking (swa=4°, initial braking speed 30 km/h) on μ=0.8 road. In the figure, these curves are: trajectory, body_yaw, body_slip_angle, longitudinal force between rear left inner wheel and ground, lateral force between front left wheel and ground, lateral force between rear left inner wheel and ground.

It can be seen from the figure that no matter the front wheel is locked, the rear wheel is locked or all is locked, the vehicle is unstable (the sideslip angle is much larger than 5°). Among them, when the front wheel is locked, the side slip of the vehicle deviates from the track up to 2m, which is very dangerous in the mountain mining area.

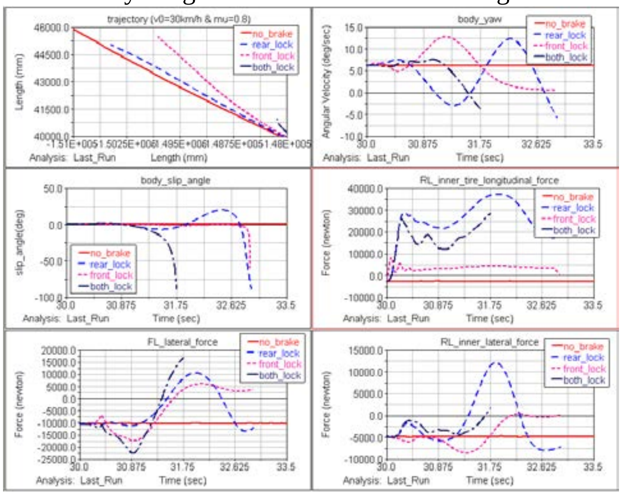

Fig. 10 Wheel lock influence on high friction road

DUMP TRUCK BRAKE REAL VEHICLE TEST

Braking deceleration, braking distance and reaction time were tested by real vehicle. The collected data have front/rear brake pressure, velocity, braking distance, etc. and by loading steel plate to simulate the full load (as shown in Fig.11 a). Test instrument have RT3100 inertial measurement system, ACME portable industrial PC, air pressure sensor (type: CYB-20S), data acquisition system (as shown in Fig.11 b). Tire pressure is as follows: right front 0.54Mpa, left front 0.54 MPa, right rear outer 0.48MPa, right rear inner 0.55MPa, left rear outer 0.47MPa, left rear inner 0.55 MPa. Full front axle load is 17620kg and rear is 30920kg. Pressure sensors installation is shown in Fig.11 c, service brake system pressure measured should be near the brake, gas pressure should achieve maximum value before test (barometric is 0.8MPa). We should start the vehicle and speeding up to the standards required and keep stability.

Fig.11 Vehicle field test

Service Braking Test

Service braking tests were conducted five times with front and rear wheels didn't lock. The 4th group test data is shown in Fig.12. There are front service brake pressure, rear service brake pressure, velocity and pedal signals respectively. Test results are shown in Table 8 for each group test.

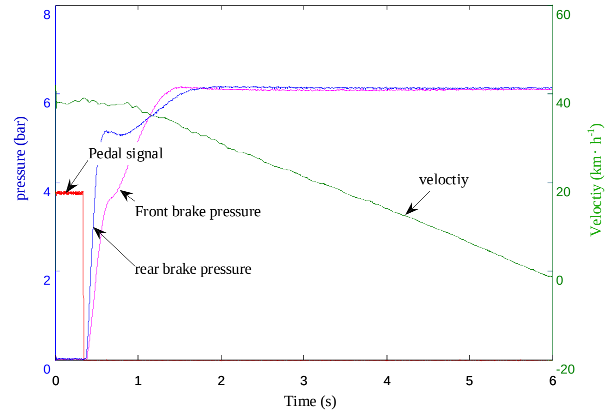

Fig.12 Truck service brake test (4th group)

Table 8. Truck service brake test

Test No.	001	002	003	004	005
Initial velocity (km/h)	36.55	37.86	38.89	37.89	40.13
front max braking pressure (×10^{-1}MPa)	6.56	6.14	6.46	6.12	6.48
rear max braking pressure (×10^{-1}MPa)	6.44	6.14	6.44	6.14	6.46
average max deceleration (g)	0.21	0.22	0.24	0.21	0.22
braking distance (m)	28.81	29.11	31.2	31.98	35.17

Emergency Brake

Restricted by test conditions, emergency brake is conducted under the front and rear pipeline in good conditions. Emergency braking test was conducted three times, the front and rear wheels didn't lock. The 2th set experimental results are shown in Fig.13, each test results are shown in Table 9.

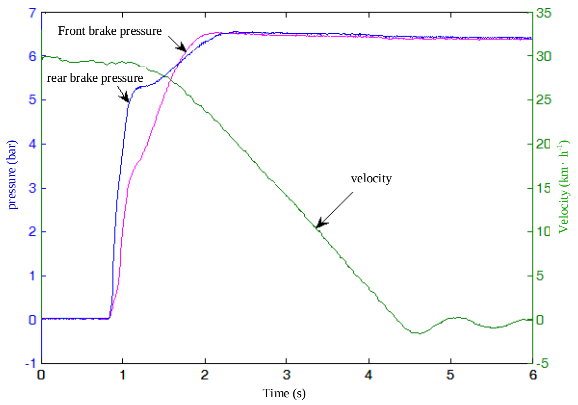

Fig.13 Emergency brake test (2th group)

Table 9. Emergency braking test (clearance elimination time 0.3s)

Test No.	001	002	003
braking original speed (km/h)	29.81	27.97	28.32
average max deceleration (g)	0.26	0.27	0.28
front max braking pressure (×10^{-1}MPa)	6.52	6.3	6.72

rear max braking pressure (× 10^{-1}MPa)	6.56	6.3	6.72
braking distance (m)	26.03	23.75	24.53

Hydraulic Retarder Downhill Ability

Since there is no 9% grade and enough long road to test, retarder working ability test was replaced with straight road. Transmission has 10 forward gears, hydraulic retarder has two gears with high and low. Using the transmission 9th gear, 3 groups were tested under hydraulic retarder high and low gear respectively. Hydraulic retarder with higher gear test results (2th group) are shown in Fig.14. There are front/rear brake pressure and velocity respectively.

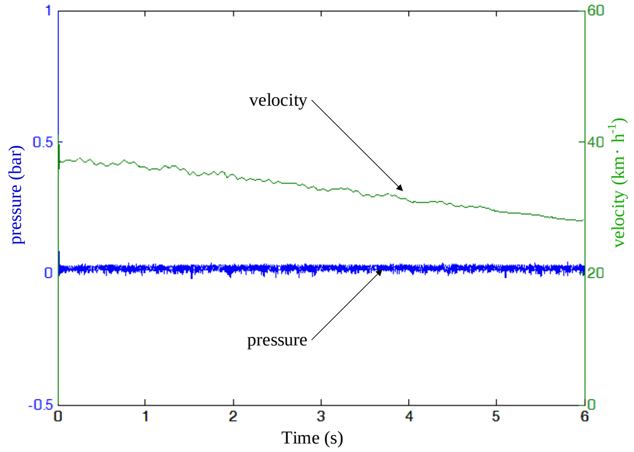

Fig.14 Retardance test results (2th group)

Braking force provided by retarder is as follows (rolling resistance is not considered).

$$F_{tr} = \delta_t m a_t \tag{15}$$

where, δ_t is rotating mass conversion coefficient, δ_t=1; m is the weight of the vehicle, 48460kg; a_t is the deceleration provided by retarder. The dump truck can drive on α_{tr} grade road under this speed.

$$\alpha_{tr} = \tan(\arcsin(\frac{F_{tr}}{mg}))\cdot 100\%$$

The hydraulic retarder test results under high and low gear are shown in Tables 10 and Table 11. From the test results, the dump truck can drive on 4.9% grade road under retarder high gear and can drive on 3.2% grade road under retarder low gear with transmission 9th gear.

Table 10. Hydraulic retarder test results (high gear)

Test No.	001	002	003
initial speed (km/h)	38.85	37.06	38.2
engine speed (r/min)	2061.5	1966.5	2027
average deceleration (g)	0.048	0.049	0.049
F_{tr} (kN)	22.8	23.3	23.3
retarder braking power (kW)	246.05	239.86	247.24
road grade can drive (%)	4.8	4.9	4.9

Table 11. Hydraulic retarder test results (low gear)

Test No.	001	002	003
initial speed (km/h)	34.89	36.99	37.33
engine speed (r/min)	1851.4	1962.8	1980.8
average deceleration (g)	0.034	0.031	0.032
F_{tr} (kN)	16.2	14.7	15.2
retarder braking power (kW)	157	151.04	157.62
road grade can drive (%)	3.4	3.1	3.2

4.4 System Response Time

Service brake system pressure response time under parking was tested three times. The 2th group test data is shown in Fig.15.

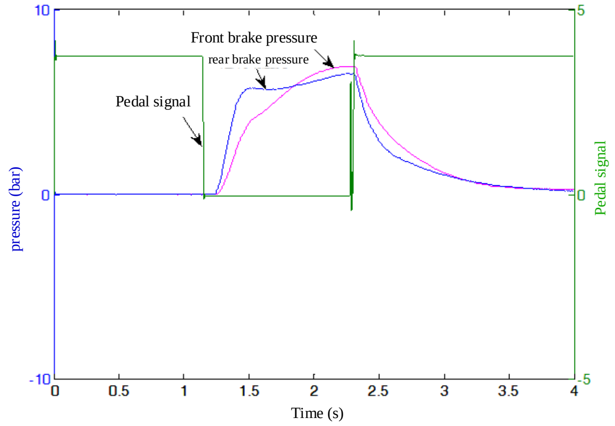

Fig.15 Service brake system pressure response time

The clearance elimination time is the duration from the moment step on the pedal to brake pressure rise moment. Pressure rise time is the duration from zero to needed maximum pressure. Service brake pressure system response time is shown in Table 12.

Table 12. Service brake pressure system response time

Test No.	001	002	003	average
front brake clearance elimination time (s)	0.076	0.1163	0.1193	0.1039
front brake pressure rise time (s)	0.9297	1.0618	1.0226	1.0047
rear brake clearance elimination time (s)	0.0533	0.0999	0.1027	0.0853
rear brake pressure rise time (s)	0.9079	1.0726	1.0392	1.0066

Emergency braking pressure system response time is shown in Table 13.

Table 13. Emergency braking pressure system response time

Test No.	001	002	003	average
front brake clearance elimination time (s)	0.2082	0.291	0.383	0.2941
front brake pressure rise time (s)	1.1824	1.1455	1.1873	1.1717
rear brake clearance elimination time (s)	0.2712	0.2842	0.361	0.3055
rear brake pressure rise time (s)	1.3666	1.4192	1.5173	1.4344

CONCLUSIONS

The accurate braking torque calculation method of mining truck pneumatic drum brake was studied firstly in this paper. Then hydro pneumatic suspension features and the tire characteristic parameters were studied. And then the vehicle virtual prototype model was established, vehicle service braking and emergency braking performance were simulated; The simulation results of braking deviation show that the rear wheel braking force is greater than that the front wheel. Under cornering braking condition, the brake deviation increases about 85 mm for each 5% difference be-tween the left and right brake forces of the front wheel; 5% difference between the left and right brake forces of the rear wheel, the brake deviation increases about 120 mm. Braking locking sideslip simulation shows that when the front wheel is locked, the side slip of the vehicle deviates from the track up to 2m, which is very dangerous in the mountain mining area. Finally, the driving downhill braking, emergency braking, hydraulic retarder ability and the system response time field experiments were carried out. The results show that the truck braking performance can also be improved. Because braking pressure rise time is slightly long, that it can be improved by gas circuit improvement (equipped with the quick-acting valve and wet-road valve, etc.), and the superiority of the improved gas path is also verified by virtual prototype simulation and real vehicle experiment. The truck braking torque can be further promoted by increasing air pressure or brake friction coefficient or brake design rationality. Through the implementation of these methods, the braking performance of the mine dump truck has been improved significantly.

ACKNOWLEDGMENTS

This research was supported by Key Scientific Research Project of Henan Province (No. 17A580003), Key scientific and technological project of Henan Province (No. 172102210022, No.182102210086), Natural Science Foundation of Henan Province of China (No.182300410265) and National Undergraduate Training Program for Innovation and Entrepreneurship (No.201710460096).

REFERENCES

Daniel L, Gheorghe A, Ionatan Teodor Z. “Analysis of truck braking system in terms of construction and operation,” Technical University of CLUJ-NAPOCA Acta Technica Napocensis, Vol. 59, No.2, pp. 209-218, (2016).

D. B. Sonawane, K. Narayan, V. S. Rao, S. C. Subramanian. “Model-Based Analysis of the Mechanical Subsystem of an Air Brake System,” International Journal of Automotive Technology, Vol. 12, No. 5, pp. 697−704, (2011)

Decheng Zhou, Guoqiang Sang, Yuchen Liu. “Mathematical model of oil and gas suspension cylinder and output force characteristics simulation analysis,” Journal of system simulation, Vol.20, No.1, pp. 220-222, (2005).

H.B.Pacejka. Tyre and Vehicle Dynamics. Butterworth-Heinemann, Oxford, UK, (2006).

Hemant L. Aghav. “Life Prediction for Vertical and Braking loading of Front Axle of Heavy-Duty Truck,” International Journal of Engineering Science and Computing, Vol. 6, No. 7, pp.8207-8211, (2016).

Li G, Pan B, Song D, et al. “Regenerative Braking Control Strategy of Hydraulic In-wheel Motor Drive System for Heavy Truck,” International Conference on Advances in Energy and Environmental Science, Zhuhai, China, (2015).

Maxym Dyachuk. “Modeling of truck's braking dynamics with ABS,” Transport Problems, Vol. 9, No. 3, pp. 21-30, (2014).

SAE J1473-90. Brake Performance-Rubber-Tired Earth-moving Machines, (1990).

Selim Hasagasioglu, Koray Kilicaslan, Orhan Atabay, Ahmet Güney. “Vehicle dynamics analysis of a heavy-duty commercial vehicle by using multibody simulation methods,” International Journal of Advanced Manufacturing Technology, Vol. 60, No. 5-8, pp.825–839, (2012).

Shimanovsky A. “Oscillations of Partially Filled Tanker Truck at Its Braking,” Engineering For Rural Development, Jelgava, (2016).

S.Mithun, S.Mariappa, Suresh Gayakwad. “Modeling and simulation of pneumatic brake system used in heavy commercial vehicle,” IOSR Journal of Mechanical and Civil Engineering, Vol.11, No. 1, pp. 01-09, (2014).

Subhajit Mahanty, Shankar C. Subramanian. “Model Based Analysis of a Heavy Commercial Vehicle with an Electropneumatic Brake towards Antilock Braking Systems,” International Conference on Vehicular Electronics and Safety, Pune, India, pp.130-135, (2009).

Wong JY. Theory of ground vehicles. John Wiley and Sons, New York, (2001).

Yibin Wang. “Mine truck brake system analysis,” Ph.D. Thesis, Jilin University, Changchun, China, (2005).

Zhang Peng. “Vehicle dynamics simulation study,” Ph.D. Thesis, Tsinghua University, Beijing, China, (2008).

礦用汽車氣壓制動系統能力虛擬樣機和實車實驗

范小彬 宋增
河南理工大學機械與動力工程學院

摘要

本文首先研究了礦用汽車空氣制動器鼓型制動器制動力矩的精確計算方法，研究了液壓氣動懸架和輪胎能力參數。設立了自卸車虛擬樣機模型，對行車制動和反應制動能力進行了模擬。制動偏差模擬結果表明，背向輪制動力大於前輪。在曲線制動條件下，前輪左右制動力差每增加 5%，制動偏差增加約 85 mm；背向輪左右制動力差每增加 5%，制動偏差增加約 120 mm。制動鎖止側滑模擬表明，前輪鎖止時，車輛側滑偏離軌道可達 2 米，在山區開採極為危險。對自卸車進行了常用制動、緊急制動、液壓緩速器、制動系統回應時間等能力現場試驗，結果表明，車輛制動能力也有了改善。由於制動壓力上升時間稍長，可通過氣路改進（配速動閥、濕路閥等），並通過虛擬樣機模擬和實車試驗驗證了改進氣路的優越程度。通過提高氣壓或制動摩擦係數或制動設計的合理程度，可以進一步提高車輛的制動力矩。通過這些方法的實施，使礦用自卸汽車的制動能力有顯著提高。